Journal of Magnetism and Magnetic Materials 401 (2016) 339–344

Contents lists available at ScienceDirect

Journal of Magnetism and Magnetic Materials

journal homepage: www.elsevier.com/locate/jmmm

Exchange bias in Ag/FeCo/Ag core/shell/shell nanoparticles due to partial oxidation of FeCo intermediate shell

Mari Takahashi, Priyank Mohan, Derrick M. Mott, Shinya Maenosono *

School of Materials Science, Japan Advanced Institute of Science and Technology, 1-1 Asahidai, Nomi, Ishikawa 923-1292, Japan

A R T I C L E I N F O

Article history:
Received 26 August 2015
Received in revised form
14 October 2015
Accepted 14 October 2015

PACS:
75.30.Et
75.75.Fk

Keywords:
Iron cobalt
Cobalt–wüstite
Exchange bias
Hybrid nanoparticles

A B S T R A C T

Recently we developed magnetic–plasmonic Ag/FeCo/Ag core/shell/shell nanoparticles for the purpose of biological applications. In these heterostructured nanoparticles, exchange bias is observed as a result of the formation of an interface between ferromagnetic FeCo and antiferromagnetic $Co_xFe_{1-x}O$ due to the partial oxidation of the FeCo intermediate shell. In this study we thoroughly characterized the surface oxide layer of the FeCo shell by XPS, XRD and SQUID magnetometer.

1. Introduction

Magnetic–plasmonic hybrid nanoparticles (NPs) have received considerable attention in recent years because they have the potential for a wide range of applications, especially in the field of biology [1–5]. We recently developed Ag/FeCo/Ag core/shell/shell NPs of mean diameter ca. ~15 nm, combining FeCo with Ag into a single hetero-nanostructure that exhibits magnetic and plasmonic properties, giving magnetic separation and imaging capability [6]. The basic design concept of the Ag/FeCo/Ag core/shell/shell hetero-nanostructure is that the Ag core provides localized surface plasmon resonance property along with having a role in suppressing oxidation of the ferromagnetic FeCo alloy shell *via* electron transfer [7] from the Ag core to the FeCo shell. The Ag outer shell also plays an important role in suppressing oxidation of the FeCo intermediate shell as well as providing a surface which is easily-modifiable through metal-thiol interactions. However, a detailed assessment of the surface oxide layer of the FeCo shell has remained unachieved, even though the oxidation of the FeCo shell dramatically affects its magnetic properties. Therefore, we performed a detailed characterization of the surface oxide layer of the FeCo intermediate shell using XPS, X-ray diffractometry (XRD), and superconducting quantum interference device (SQUID) magnetometer and found that the oxide layer is $Co_xFe_{1-x}O$ cobalt–wüstite phase which is manifested especially by exchange bias as a result of the formation of an interface between ferromagnetic (FM) FeCo and antiferromagnetic (AFM) $Co_xFe_{1-x}O$ within the FeCo shell.

2. Experimental section

2.1. Synthesis of Ag/FeCo/Ag NPs

Ag/FeCo/Ag NPs were synthesized following the previously reported method [6,8]. Two types of stock solutions were prepared in advance. The first stock solution contained 0.2 mmol of iron(III) acetylacetonate [$Fe(acac)_3$] (Sigma-Aldrich), 0.2 mmol of cobalt(II) acetylacetonate [$Co(acac)_2$] (Sigma-Aldrich), 1 mL of oleylamine (OLA) (Sigma-Aldrich) and 2 mL of toluene (Wako Pure Chemical). The second stock solution contained 0.1 mmol of silver nitrate ($AgNO_3$) (Sigma-Aldrich), 1 mL of OLA and 1 mL of toluene. First 0.1 mmol of $AgNO_3$, 1.0 mmol of 1,2-hexadecanediol (HDD) (Sigma-Aldrich), 10 mmol of OLA, 8 mmol of oleic acid (OA) (Sigma-Aldrich) and 10 mL of tetraethyleneglycol (TEG) (Sigma-Aldrich) were put into a three neck flask. Then, a trap sphere which was connected to a condenser was connected to the three neck flask. A thermocouple and a Pasteur pipette from which Ar gas was supplied were also dipped into the reaction solution in the three

---

* Corresponding author. Fax: +81 761 51 1625.
E-mail address: shinya@jaist.ac.jp (S. Maenosono).

http://dx.doi.org/10.1016/j.jmmm.2015.10.050

neck flask. The reaction solution was degassed with Ar gas at room temperature for 5 min then the temperature was increased to 100 °C and kept for 10 min. After waiting 10 min the temperature was increased to 250 °C. During increasing the temperature the first stock solution was injected into the reaction solution at 170 °C and the second stock solution was also injected at 250 °C. Immediately after the second injection the temperature was set to 230 °C and held for 15 min. When the reaction was completed the temperature was decreased and the reaction solution was divided into two centrifuge tubes. Acetone (Kanto Chemical) was added into the two centrifuge tubes to make the total volume 45 mL and the tubes were centrifuged at 4500 rpm for 5 min. After discarding the supernatant, 400 μL of hexane (Kanto Chemical) was added into each tube to disperse the precipitated NPs. 200 μL of dispersed NPs were taken from each tube and put into two new tubes. Acetone was added to the four tubes to make the total volume 45 mL and was centrifuged again with the same conditions. Finally, the precipitated NPs were dried in a vacuum drying system after discarding the supernatant. As synthesized Ag/FeCo/Ag NPs were immediately measured by XRD within 30 min after synthesis. The NPs were also inserted into the vacuum chambers in SQUID and XPS instruments within 90 min after synthesis. The samples were kept in a vacuum drying system as much as possible excluding for the sample preparation.

2.2. Synthesis of $Co_xFe_{1-x}O$ NPs

Synthesis of $Co_xFe_{1-x}O$ NPs was followed in a similar way to the previous reports [6,8]. First 0.2 mmol of $Fe(acac)_3$, 0.2 mmol of $Co(acac)_2$, 1.0 mmol of HDD, 10 mmol of OLA, 8 mmol of OA and 10 mL of TEG were put into a three neck flask. Then, the reaction solution was degassed with Ar gas at room temperature for 5 min. After that the temperature was increased to 100 °C and kept for 10 min. Next, the temperature was increased again up to 290 °C and kept at that temperature for 20 min. After the reaction, the reaction solution was cooled down and separated into two centrifuge tubes, followed by the addition of acetone to make the total volume 45 mL. Then the centrifuge tubes were kept for 2 h to precipitate the products naturally. After that, the tubes were centrifuged at 4500 rpm for 5 min and the products were dried in a vacuum drying system after discarding the supernatant.

3. Results and discussion

3.1. Morphology and surface chemical states

Fig. 1 shows transmission electron microscope (TEM) images of as-synthesized Ag/FeCo/Ag core/shell/shell NPs (taken on a Hitachi H-7650 instrument operated at 100 kV). The mean size of the NPs was measured to be 14.6 ± 2.1 nm (n=367) from the TEM images. Fig. 2 shows Fe 2p and Co 2p XPS spectra for Ag/FeCo/Ag NPs obtained using a high-performance X-ray photoelectron spectroscopy (a Shimadzu Kratos AXIS-ULTRA DLD system) instrument. Note that as-synthesized NPs were immediately inserted into the XPS chamber followed immediately by evacuation. The duration of exposure of the NPs to air was minimized to less than 1 h after the completion of the synthesis. To precisely analyze the chemical states of the NPs, the XPS spectra were deconvoluted into the respective chemical species using a Gaussian–Lorentzian mixed function by XPSPEAK41 software. The Fe 2p spectra were deconvoluted into Fe^0, Fe^{2+}, Fe^{3+}, high-binding energy (BE) surface structures (abbreviated 'Fe surface' in Table 1) and satellite peaks. The Co 2p spectra were deconvoluted into Co^0, Co^{2+}, Co^{3+} and satellite peaks. The BEs of each peak for Ag/FeCo/Ag NPs are summarized in Table 1. The atomic ratio between Fe and Co was determined to be Fe:Co=67:33. On the other hand, the Fe:Co composition measured by inductively coupled plasma optical emission spectroscopy (ICP-OES; Shimadzu ICPS-7000) was near equiatomic (Fe:Co=55:45). This discrepancy is caused because there is a composition gradient within the FeCo shell in which Co is rich near the Ag core while Fe is rich on the surface of the FeCo shell. The relative proportions of oxidation states of each species ($Fe^0/Fe^{2+}/Fe^{3+}$ and $Co^0/Co^{2+}/Co^{3+}$) for Ag/FeCo/Ag NPs determined by XPS are $Fe^0/Fe^{2+}/Fe^{3+}$ = 15:56:29 and $Co^0/Co^{2+}/Co^{3+}$ = 23:47:30. As can be seen, the relative proportions of divalent species (Fe^{2+} and Co^{2+}) are the highest.

3.2. Crystalline phase

For the latter argument, we also synthesized $Co_xFe_{1-x}O$ NPs by polyol method. Fig. 3a shows a TEM image of $Co_xFe_{1-x}O$ NPs whose diameter is 5.6 ± 1.2 nm (n=356). ICP-OES analysis revealed the atomic ratio between Fe and Co is Fe:Co=52:48, confirming that x=0.5 for the resulting $Co_xFe_{1-x}O$ NPs. The XRD pattern of the $Co_{0.5}Fe_{0.5}O$ NPs obtained using a Rigaku MiniFlex600 instrument operated in reflection geometry at room

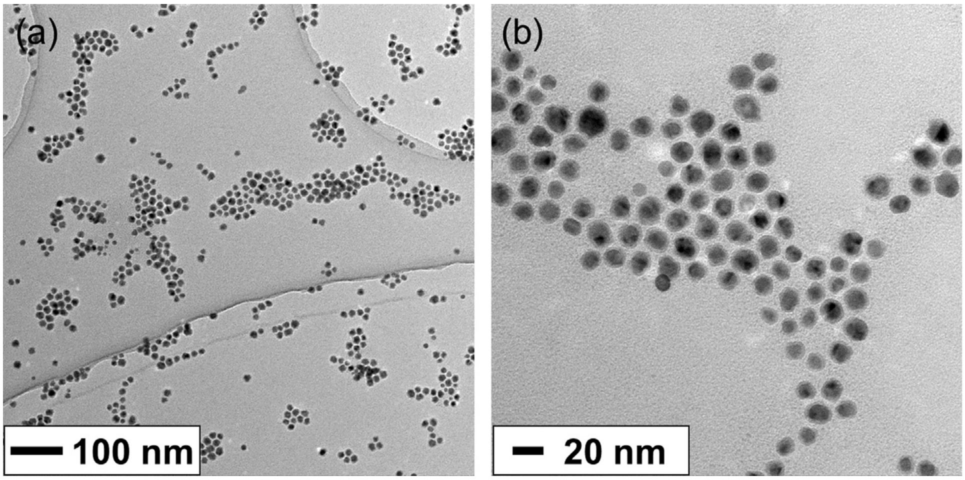

Fig. 1. (a) Low and (b) high magnification TEM images of as-synthesized Ag/FeCo/Ag NPs.